Wireless Power Transfer

cambridge.org/wptcup

Research Article

Cite this article: Minnaert B, Mongiardo M, Costanzo A, Mastri F (2020). Maximum efficiency solution for capacitive wireless power transfer with *N* receivers. *Wireless Power Transfer* **7**, 65–75. https://doi.org/10.1017/wpt.2020.9

Received: 2 October 2019
Revised: 12 January 2020
Accepted: 18 February 2020
First published online: 19 March 2020

Key words:
Capacitive; components and circuits; efficiency and optimization

Author for correspondence:
Ben Minnaert, Odisee University College of Applied Sciences, Ghent, Belgium.
E-mail: ben.minnaert@odisee.be

CAMBRIDGE UNIVERSITY PRESS

Maximum efficiency solution for capacitive wireless power transfer with *N* receivers

Ben Minnaert[1], Mauro Mongiardo[2], Alessandra Costanzo[3] and Franco Mastri[3]

[1]Odisee University College of Applied Sciences, Ghent, Belgium; [2]Department of Engineering, University of Perugia, Perugia, Italy and [3]Department of Electrical, Electronic and Information Engineering Guglielmo Marconi, University of Bologna, Bologna, Italy

Abstract

Typical wireless power transfer (WPT) systems on the market charge only a single receiver at a time. However, it can be expected that the need will arise to charge multiple devices at once by a single transmitter. Unfortunately, adding extra receivers influences the system efficiency. By impedance matching, the loads of the system can be adjusted to maximize the efficiency, regardless of the number of receivers. In this work, we present the analytical solution for achieving maximum system efficiency with any number of receivers for capacitive WPT. Among others, we determine the optimal loads and the maximum system efficiency. We express the efficiency as a function of a single variable, the system kQ-product and demonstrate that load capacitors can be inserted to compensate for any cross-coupling between the receivers.

Introduction

Wireless power transfer (WPT) eliminates the need for physical connections for charging a device. Power is transferred wirelessly from a transmitter to a receiver. Compared to traditional wired charging, WPT has several advantages, including improved convenience and user experience, higher durability and robustness, and increased safety in hazardous industrial environments [1–3]. Due to the benefits, the global market for WPT devices is growing rapidly. More than 600 million units (transmitters and receivers) were shipped in 2018, a growth of 37% compared to 2017 [4].

Most WPT devices on the market charge only a single receiver at a time. However, it can be expected that the need will arise to charge multiple devices at once, i.e. to simultaneously charge multiple receivers by a single transmitter. But adding extra receivers to the WPT system influences the system efficiency. In order to obtain an efficient energy transfer, the operating conditions of the system have to change depending on the number of receivers and their properties.

By impedance matching, the system can be adapted to work optimally for multiple receivers. However, this requires an analytical solution for achieving maximum system efficiency, valid for a set-up with *any* number of receivers. This *maximum efficiency solution* for *N* receivers was already reported [5–11] for the currently most prevalent WPT technology, *inductive* WPT, but as far as we know, no solution was presented yet for *capacitive* WPT. Both methods are near-field (non-radiative) techniques, but *inductive* WPT uses mainly *magnetic* coupling to transfer energy, whereas the *capacitive* technique employs *electric* coupling.

The wireless link in a capacitive wireless power transfer (CWPT) system is established by metal plates, often coated with a dielectric material. Different configurations are possible for the plates [12]:

- the four-plate structure is typically applied: two conducting plates at the transmitter's side and two at the receiver's side (Fig. 1).
- the two-plate structure where two plates realize the wireless link, and a conducting (wired) link (e.g. the ground) is applied as return path [13, 14].
- the four-plate stacked structure: the two transmitter plates are placed close to each other to increase the self-capacitance and decrease the external capacitances. The same is done with the two receiver plates [15, 16].
- the six-plate structure to reduce electric field emissions [17].

The principle of each configuration is the same: by applying an alternating voltage at the transmitter's plates, an electric field is created. This varying electric field realizes electric (also called capacitive) coupling with the receiver's plates, where current is generated. Since

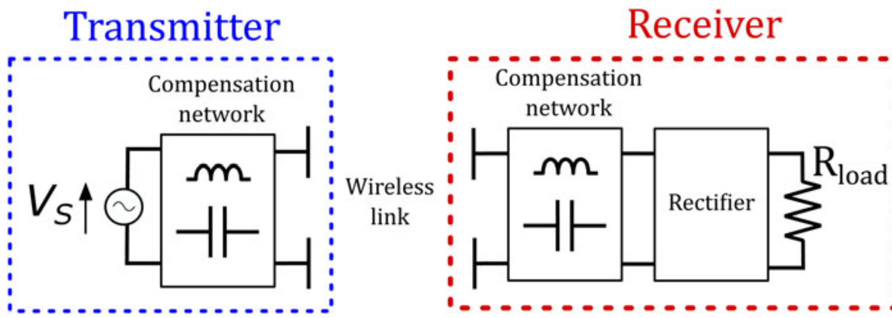

Fig. 1. A general four-plate CWPT system: the energy from an AC-signal V_S is transferred to the load R_{load}. The four conducting plates constitute the wireless link. Compensation networks at the transmitter and/or receiver side are present to realize resonance. A rectifier converts the AC-signal to DC.

the transmitter and receiver plates are at a certain distance positioned opposite to each other, energy is transferred wirelessly from a transmitter to a receiver.

The coupling between a transmitter and a receiver is dependent on the distance, the plate area, and the permittivity of the material between the plates. Since the permittivity of air is small, the coupling of a CWPT system will be low. In order to increase the coupling, a resonant circuit is constructed by adding a compensation network, which is usually an inductor, or a combination of inductors and capacitors (Fig. 1). References [12] and [18] give a comprehensive overview of different types of compensation networks. By operating the system at the corresponding resonant frequency, high voltages are generated at the plates, resulting in a higher electric coupling between a transmitter and a receiver. Usually, high frequencies (in the order of a few MHz) are necessary to bridge larger distances of, e.g. 10 cm.

This highlights the disadvantages of CWPT compared to inductive WPT. Large plates, high frequencies, and high voltages are necessary for long distances. Moreover, the high electric field between the transmitter and receiver plates can cause safety concerns [19, 20].

However, compared to inductive WPT, it also has some advantages [16, 20–23], for example:

- CWPT is able to transfer power through metal objects. Moreover, power losses are less than for a comparable inductive WPT system when metal objects are nearby.
- A CWPT system will usually produce less heat than an inductive WPT system.
- The electric field lines of a CPWT link are less outstretched as the magnetic field lines of an inductive WPT link.
- CWPT is often less expensive and less heavy than a comparable inductive WPT system.

CWPT is especially suited for short-range applications, e.g. integrated circuits [12, 24], portable electronics [25, 26], consumer applications [27], and biomedical implants [28, 29].

The above examples are located in the low to midrange power levels, from a few watts to 100 W. However, CWPT also allows for high power transfer, well above kilowatt level (at a short distance), and can be used by, e.g. electric vehicles [30] and automatic guided vehicles [31].

In this work, we present the analytical solution for a capacitive WPT system with an arbitrary number of receivers. In a CWPT system, the electric field is generated by applying an alternating voltage to conducting transmitter plates. At a certain distance from the transmitter plates, the receiver plates capture the energy from the electric field to generate current and power a load. To date, most applications focus on the energy transfer to a single receiver. However, since the plates of a CWPT link are simple and cheap electrodes, multiple receivers can be powered at once by a single transmitter: large transmitter plates can cover multiple smaller receiver plates (Fig. 2). One could, for example, imagine that low-power consumer devices are simultaneously charged on a large surface area.

Another example application is the wireless charging of electric taxis while queuing: as the taxis await their customers at a designated area, a transmitter plate below the ground charges the vehicles wirelessly (Fig. 3). The return path for the circuit is delivered by the chassis of the vehicle [13]. Although this example is far from being implemented in real life, due to practical and safety concerns [12], CWPT technology is rapidly developing in recent years, and we hope an exact solution to the multiple receiver problem might contribute to its progress.

The main idea of this work is that we determine the receivers' loads for a CWPT system with one transmitter and N receivers that maximize the system efficiency (also called the power gain). For different receivers and different coupling strengths, other load values apply that maximize the system efficiency. Often, the value of the loads varies when the system is operational. In practice, impedance matching networks are inserted between the loads and the output ports of the receiver in order to adapt the load to their optimal value. More specifically, our contributions are as follows:

- We compose an equivalent circuit for a general CWPT system with one transmitter and N receivers ("Equivalent circuit" section).
- We analytically determine the input power, output power, and efficiency of this equivalent circuit as a function of its components ("Power and efficiency of the CWPT system" section).
- We calculate the optimal current–voltage relationships at the transmitter and receiver ports, necessary to realize maximal efficiency of the system ("Maximum efficiency configuration" section). From these expressions, we derive closed-form expressions for the optimal loads and the maximum efficiency ("Maximum efficiency configuration" section).
- We demonstrate that we can compensate for the coupling between the receivers by adding specific capacitors. We discuss the optimal loads and describe the maximum efficiency as a function of a single variable, the system kQ-product ("Discussion" section).
- Finally, we verify the analytical derivation by numerical circuit simulation for an example CWPT system with one transmitter and three receivers ("Numerical verification" section).

We want to stress that maximizing the efficiency does not maximize the amount of power transferred to the load, nor does it realize a uniform power distribution among the different receivers. Different load values will apply for maximizing the

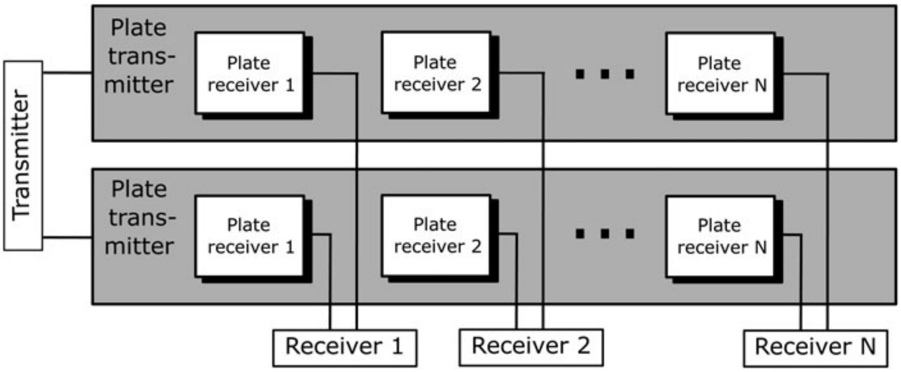

Fig. 2. Example configuration of the transmitter and receiver plates of a capacitive wireless link with one transmitter and *N* receivers. Large transmitter plates allow the energy transfer to multiple smaller receiver plates.

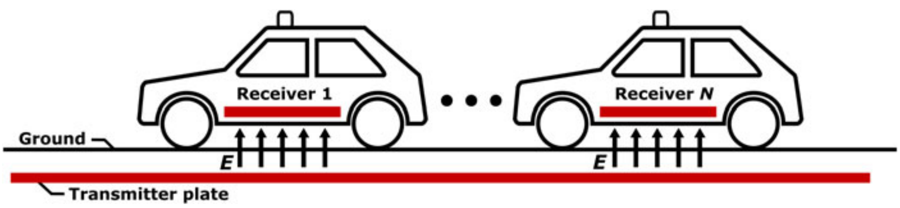

Fig. 3. A futuristic example application of CWPT with multiple receivers: as *N* (electric) taxis are queuing at a designated area, a transmitter plate below the ground transfers energy to a receiver plate at the bottom of the vehicles, by means of the electric field *E*. The electrical circuits are omitted on the figure for clarity.

amount of output power [11], or realizing a uniform power distribution [32].

Equivalent circuit

We consider a CWPT system with one transmitter and N receivers. Figure 4 shows the equivalent circuit of the wireless link between the transmitter (on the left, subscript 0) and the N receivers (on the right, subscripts 1 to N). This system can be considered as a linear reciprocal $(N+1)$-port network at the ports with peak voltage phasors V_i and peak current phasors I_i, as defined in the figure ($i = 0,\ldots, N$). We use the following notation to represent the real and imaginary parts of the phasors: $V_i = V_i^{re} + jV_i^{im}$ and $I_i = I_i^{re} + jI_i^{im}$.

The $(N+1)$-port network is fully characterized by its admittance matrix $\boldsymbol{Y}$, indicated by the dashed rectangle. The efficiency η is dependent on $\boldsymbol{Y}$ and on the loads at the ports. In this work, we consider the input current I_0 and the CWPT link as given, i.e. the admittance matrix $\boldsymbol{Y}$ is fixed.

In order to maximize the power transfer efficiency η of the wireless link, we must find the optimal values for the loads at the output ports for a given input. Since we can express the load admittance at the ports by the current-to-voltage ratios, we focus on I_i and V_i at the ports, and hide the remote electronics external to the wireless link (actual passive loads, matching networks, power source, rectifiers, etc.).

With Kirchhoff's current laws, the relations between the voltages and currents of the $(N+1)$-port network are obtained:

$$\boldsymbol{I} = \boldsymbol{Y} \cdot \boldsymbol{V}. \tag{1}$$

The $(N+1) \times 1$ matrices $\boldsymbol{V}$ and $\boldsymbol{I}$ are defined as

$$\boldsymbol{V} = \begin{bmatrix} V_0 \\ V_1 \\ V_2 \\ \vdots \\ V_N \end{bmatrix}, \boldsymbol{I} = \begin{bmatrix} I_0 \\ I_1 \\ I_2 \\ \vdots \\ I_N \end{bmatrix}. \tag{2}$$

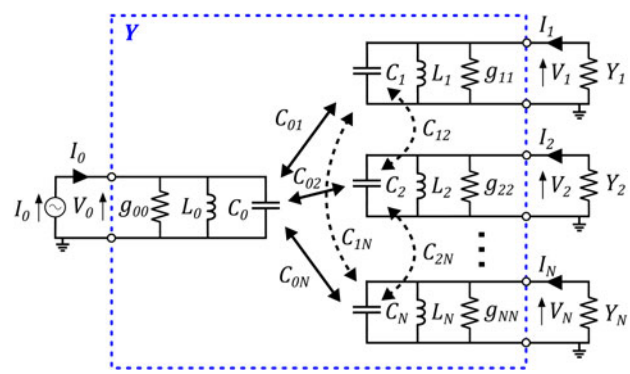

Fig. 4. Equivalent circuit of a capacitive wireless power transfer system with one transmitter (left) and *N* receivers (right). The (desired) electric coupling between a transmitter and a receiver is represented by the full arrows, characterized by the mutual capacitances C_{0n} ($n = 1,\ldots, N$). An undesired electric coupling is present between the receivers, indicated by the dashed arrows.

The losses in the circuit are represented by the parallel conductances $g_{00}, g_{11}, \ldots, g_{NN}$.

The (desired) electric coupling is described by the mutual capacitance C_{0n} ($n = 1,\ldots, N$) between the transmitter capacitance C_0 and the receivers' capacitances C_n [33, 34].

An undesired electric coupling can be present between the receivers, e.g. a non-zero mutual capacitance C_{12} between the first and the second receiver. Even though in many practical systems, the coupling between the receivers is small, we will take into account this cross-coupling for our analysis: we will assume a non-negligible electric coupling between all receivers.

The coupling factor k_{ij} between circuit i and j ($i, j = 0, \ldots, N$) is defined as [33, 34]:

$$k_{ij} = \frac{C_{ij}}{\sqrt{C_i C_j}}. \tag{3}$$

Resonance shunt inductors L_i are added in parallel to each circuit, given by $(i = 0,\ldots, N)$:

$$L_i = \frac{1}{\omega_0^2 C_i}, \tag{4}$$

with ω_0 the operating angular frequency of the CWPT system. We could also opt for series inductances instead of shunt inductances to realize resonance, but the shunt configurations simplify the calculations and allow for a better understanding of the results. The methodology of the theoretical analysis remains the same for both topologies.

At the frequency ω_0, the admittance matrix $\boldsymbol{Y}$ is given by

$$\boldsymbol{Y} = \begin{bmatrix} g_{00} & -jb_{01} & -jb_{02} & \cdots & -jb_{0N} \\ -jb_{01} & g_{11} & -jb_{12} & \cdots & -jb_{1N} \\ -jb_{02} & -jb_{12} & g_{22} & \cdots & -jb_{2N} \\ \vdots & \vdots & \vdots & \ddots & \vdots \\ -jb_{0N} & -jb_{1N} & -jb_{2N} & \cdots & g_{NN} \end{bmatrix}, \tag{5}$$

with $b_{ij} = \omega_0 C_{ij}$. Due to the reciprocal network, $\boldsymbol{Y}$ is symmetric: $b_{ij} = b_{ji}$.

We want to stress that Fig. 4 does not correspond to the physical structure of a CWPT system. It represents an approximate equivalent circuit of the wireless link [33–36] and neglects the series resistances for the inductor losses. However, for the purpose of this work, the given equivalent circuit allows for a lucid analytical model that provides a first-order estimation of a CWPT system with one transmitter and an arbitrary number of receivers.

Power and efficiency of the CWPT system

By applying the circuit model, we determine the analytical expressions for the input and output power of the above equivalent circuit, representing a CWPT system with one transmitter and N receivers. From the input and output power, the power transfer efficiency is derived.

Input power

The input power P_{in} is given by:

$$P_{in} = \frac{1}{2}\Re(V_0 I_0^*), \tag{6}$$

with I_0^* the complex conjugate of I_0, and $\Re(V_0 I_0^*)$ the real part of $V_0 I_0^*$. Without loss of generality, we choose V_0 as the reference phasor, i.e. V_0 is purely real: $V_0 = V_0^{re}$. The expression reduces to:

$$P_{in} = \frac{1}{2} V_0^{re} I_0^{re}. \tag{7}$$

From (1), we find the input power P_{in} as a function of the characteristics of the network and the port voltages:

$$P_{in} = \frac{V_0^{re}}{2}\left[g_{00} V_0^{re} + \sum_{n=1}^{N} b_{0n} V_n^{im}\right]. \tag{8}$$

Output power

The output power P_n at port n $(n = 1,\ldots, N)$ equals, taking into account the passive sign convention:

$$P_n = -\frac{1}{2}\Re(V_n I_n^*) = -\frac{1}{2}(V_n^{re} I_n^{re} + V_n^{im} I_n^{im}). \tag{9}$$

The total output power P_{out} is defined as:

$$P_{out} = \sum_{n=1}^{N} P_n. \tag{10}$$

From (1) and (9), the output power P_{out} follows as a function of the characteristics of the network and the port voltages:

$$P_{out} = -\frac{1}{2}\left[\sum_{n=1}^{N} g_{nn}[(V_n^{re})^2 + (V_n^{im})^2] - V_0^{re}\sum_{n=1}^{N} b_{0n} V_n^{im} + \sum_{\substack{n,m=1 \\ n \neq m}}^{N} b_{nm}(V_n^{re} V_m^{im} - V_n^{im} V_m^{re})\right]. \tag{11}$$

Efficiency

The power gain or efficiency η of the CWPT system is defined as:

$$\eta = \frac{P_{out}}{P_{in}}, \tag{12}$$

with P_{in} and P_{out} given by (8) and (11). Consequently, we have expressed the efficiency η as a function of the characteristics of the network and the port voltages.

Maximum efficiency configuration

In the previous section, the general expression for the efficiency of the CWPT system was determined. We now determine the current–voltage relationships at the ports that maximize the system efficiency η, i.e. that maximize expression (12). We use the notation η_{max} for the value of the maximum efficiency. We start by calculating the port voltages that realize η_{max}.

Optimal port voltages

In order to find the port voltages for which the efficiency η is maximized, we apply the first-order necessary condition [10, 37], for $n = 1,\ldots, N$:

$$\frac{\partial \eta}{\partial V_n^{re}} = 0, \tag{13}$$

$$\frac{\partial \eta}{\partial V_n^{im}} = 0. \tag{14}$$

Solving this system of $2n$ equations gives us the solution for the voltages V_n $(n = 1,\ldots, N)$ in the maximum efficiency configuration. Solving the system directly is very complicated. We will therefore solve the system indirectly.

By applying the quotient rule for derivatives and (12), the system can be rewritten as:

$$P_{in}\frac{\partial P_{out}}{\partial V_n^{re}} - P_{out}\frac{\partial P_{in}}{\partial V_n^{re}} = 0, \quad (15)$$

$$P_{in}\frac{\partial P_{out}}{\partial V_n^{im}} - P_{out}\frac{\partial P_{in}}{\partial V_n^{im}} = 0. \quad (16)$$

Taken into account (8) and (11), the system reduces to:

$$P_{in} g_{nn} V_n^{re} = 0, \quad (17)$$

$$P_{in}\left(-g_{nn}V_n^{im} + \frac{1}{2}b_{0n}V_0^{re}\right) - \frac{1}{2}P_{out}b_{0n}V_0^{re} = 0. \quad (18)$$

Finally, with (12), we find the solution for the optimal port voltages $V_n^{opt} = V_n^{re,opt} + jV_n^{im,opt}$ $(n = 1,\ldots, N)$, i.e. the port voltages that realize maximum efficiency η_{max}:

$$V_n^{re,opt} = 0, \quad (19)$$

$$V_n^{im,opt} = \frac{b_{0n}}{2g_{nn}}(1-\eta_{max})V_0^{re}. \quad (20)$$

Note that the voltages are not only a function of the known characteristics of the network and the input voltage V_0^{re}, but also of the – at this point – still unknown value of η_{max}.

Optimal input and output power

Substituting (19) and (20) in (8) and (11) results in the following expressions for the input power P_{in}^{opt} and output power P_{out}^{opt} at the maximum efficiency solution:

$$P_{in}^{opt} = \frac{1}{2}(V_0^{re})^2 g_{00}\left[1 + \frac{(1-\eta_{max})}{2}\alpha_N^2\right], \quad (21)$$

$$P_{out}^{opt} = \frac{1}{8}(V_0^{re})^2 g_{00}(1-\eta_{max})(1+\eta_{max})\alpha_N^2, \quad (22)$$

where we introduced the following notation:

$$\alpha_N^2 = \sum_{n=1}^{N}\alpha_n^2, \quad (23)$$

with

$$\alpha_n = \frac{b_{0n}}{\sqrt{g_{00}g_{nn}}}. \quad (24)$$

We call α_n the *extended kQ-product* of the link between the transmitter and the nth receiver, as defined by [9, 38, 39]. We name α_N the *system kQ-product*, analogous to [9, 40, 41]. We will discuss these parameters in "Discussion" section.

Again note that the powers are dependent on the known characteristics of the network, the input voltage V_0^{re}, and the still unknown value of η_{max}.

Maximum efficiency

We now determine the maximum efficiency η_{max}. Substituting (21) and (22) in (12) results in a quadratic equation in η_{max}:

$$\eta_{max}^2 - \left(2 + \frac{4}{\alpha_N^2}\right)\eta_{max} + 1 = 0. \quad (25)$$

Solving the quadratic equation gives two solutions:

$$\eta_{max,1} = \frac{\sqrt{1+\alpha_N^2}-1}{\sqrt{1+\alpha_N^2}+1} \quad (26)$$

and

$$\eta_{max,2} = \frac{\sqrt{1+\alpha_N^2}+1}{\sqrt{1+\alpha_N^2}-1}. \quad (27)$$

Since $0 \le \eta_{max} \le 1$, equation (27) is physically not possible. The maximum efficiency η_{max} is given by equation (26), which can also be written as:

$$\eta_{max} = 1 - \frac{2}{1+\sqrt{1+\alpha_N^2}}. \quad (28)$$

We have expressed η_{max} as a function of the characteristics of the network only. In this way, also the optimal voltages, input and output power are determined as a function of the characteristics of the network.

Optimal port currents

In the maximum efficiency configuration, the port current $I_n^{opt} = I_n^{re,opt} + jI_n^{im,opt}$ can be determined from (1), (19), and (20). We find:

$$I_n^{re,opt} = g_{nn}V_n^{opt}, \quad (29)$$

$$I_n^{im,opt} = -\sum_{\substack{m=0 \\ m\neq n}}^{N} b_{nm}V_m^{opt}. \quad (30)$$

Optimal load admittances

Finally, we determine the required values for the admittance loads at the output ports to realize maximum efficiency. The optimal load at output port n $(n = 1,\ldots, N)$ is given by:

$$Y_n^{opt} = G_n^{opt} + jB_n^{opt} = -\frac{I_n^{opt}}{V_n^{opt}}. \quad (31)$$

With (29) and (30), we obtain:

$$Y_n^{opt} = -g_{nn} + \frac{j}{V_n^{opt}} \sum_{\substack{m=0 \\ m \neq n}}^{N} b_{nm} V_m^{opt}. \tag{32}$$

With $v_0 = V_0^{re}$, (19) and (20), we find:

$$Y_n^{opt} = g_{nn} \frac{1+\eta_{max}}{1-\eta_{max}} + j \frac{g_{nn}}{b_{0n}} \sum_{\substack{m=1 \\ m \neq n}}^{N} \frac{b_{0m} b_{nm}}{g_{mm}}. \tag{33}$$

Substituting (28) in the above expression results in the optimal load admittance $Y_n^{opt} = G_n^{opt} + jB_n^{opt}$ at each output port n ($n = 1, \ldots, N$) as a function of the characteristics of the network (i.e. the elements of the admittance matrix $\boldsymbol{Y}$):

$$G_n^{opt} = g_{nn}\sqrt{1+\alpha_N^2}, \tag{34}$$

$$B_n^{opt} = \frac{g_{nn}}{b_{0n}} \sum_{\substack{m=1 \\ m \neq n}}^{N} \frac{b_{0m} b_{nm}}{g_{mm}}. \tag{35}$$

The optimal susceptances are always positive, i.e. the optimal complex loads are capacitors. The value of the optimal load capacitors $C_{load,n}^{opt}$ is:

$$C_{load,n}^{opt} = \frac{g_{nn}}{b_{0n}\omega_0} \sum_{\substack{m=1 \\ m \neq n}}^{N} \frac{b_{0m} b_{nm}}{g_{mm}}. \tag{36}$$

Discussion

We discuss the analytical results from the previous section, in particular the optimal values of the loads, the maximum efficiency, and the system kQ-product.

Both the optimal load conductance G_n^{opt} and load capacitance $C_{load,n}^{opt}$ of receiver n are proportionate to the parasitic conductance g_{nn} of the nth receiver. The load capacitance of receiver n is inversely proportional to the coupling between the transmitter and the nth receiver.

When the coupling is high ($\alpha_N \gg 1$), the optimal conductances approximate to:

$$G_n^{opt} = g_{nn}\alpha_N. \tag{37}$$

We now look into the influence of cross-coupling, i.e. the mutual coupling between each of the receivers. This coupling is represented by the parameter b_{nm} for $n, m = 1, \ldots, N$.

- According to equation (34), the optimal conductances G_n^{opt} are independent of the coupling between the receivers. As well for coupled as uncoupled receivers, the optimal conductances G_n^{opt} assume the same value.

Table 1. Numerical examples of the required extended system kQ-product α_N to achieve a given maximum efficiency η_{max}

α_N	0	2.8	3.9	5.6	9	19	39	100	200
η_{max}[%]	0	50	60	70	80	90	95	98	99

- From equation (36), it follows that, when there is no coupling between any of the receivers (i.e. $b_{nm} = 0$ for $n, m = 1, \ldots, N$), the optimal load capacitors are absent. In other words, the optimal loads to maximize the efficiency of the CWPT system are purely real.
- The cross-coupling between the receivers does not influence the maximum efficiency η_{max}. Indeed, the parameter b_{nm} ($n, m = 1, \ldots, N$) is not present in equations (23), (24), and (28). This does not imply that the *efficiency* is not influenced by cross-coupling for a *general* CWPT system; it is the *maximum* efficiency that is invariant for cross-coupling for an *optimized* system toward efficiency, i.e. where the loads satisfy equations (34) and (36).
- Combining the above observations, we can conclude that the optimal load capacitances $C_{load,n}^{opt}$ eliminate the influence of the cross-coupling; the maximum efficiency of a CWPT system with no cross-coupling equals the maximum efficiency of a CWPT system with cross-coupling and optimized load capacitors. For both the uncoupled as the coupled system, the optimal load conductances are the same.

The expression for the maximum efficiency η_{max} is given by (28). The second term is the measure for the losses of the CWPT system. This term is only dependent on a single scalar variable, i.e. α_N. Table 1 gives some numerical values for their relationship. The efficiency approaches unity for increasing α_N.

It is a property of *any* reciprocal transfer system that the efficiency can be expressed as a function of a single variable [38]. For WPT systems with a single receiver, this one variable is often called the *extended kQ-product*, since it corresponds to the kQ-product which is often used as a figure of merit [9, 38, 39].

Since the value of α_N determines the maximum efficiency of the CWPT system with N receivers, we call this parameter the *system kQ-product*. From equation (23), we can conclude that the square of the system kQ-product equals the sum of the squares of the kQ-products of each individual transmitter–receiver link. The figure of merit α_n for each individual transmitter–receiver link can thus provide insight in the figure of merit α_N for the entire system: measuring the kQ-products of the individual transmitter–receiver links allows an estimation of the total system efficiency.

The extended kQ-product α_n, and thus also the system kQ-product α_N, depends on the coupling between the transmitter and each receiver, but is independent on the coupling between the receivers mutually.

Notice the reasoning for naming the parameter α_N the system kQ-product: the expression for the maximum efficiency for a single link inductive or a single link capacitive WPT system is identical to our derived expression for a CWPT system with N receivers [9, 39, 42]. It only differs in the value of the single variable.

In this way, the CWPT system with N receivers can be represented by an equivalent circuit with the same transmitter, and only one receiver with b'_{0n} and g'_{nn} chosen such that

$$\alpha_N = \frac{b'_{0n}}{\sqrt{g_{00}g'_{nn}}}. \tag{38}$$

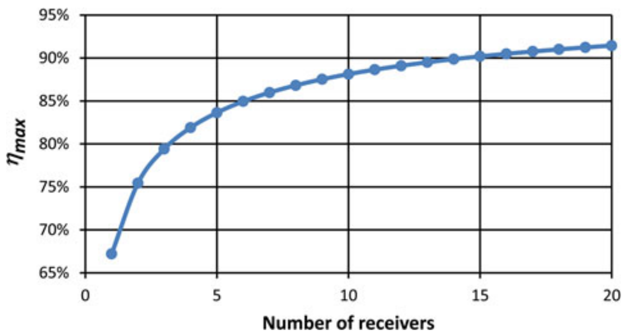

Fig. 5. The maximum achievable efficiency η_{max} as a function of the number of receivers, for identical receivers and transmitter–receiver coupling ($\alpha_n = 5$).

From (23), (24), and (28), it follows that the higher the system kQ-product α_N, the higher the efficiency of the system. This implies that, in order to increase the efficiency of the system, the following statements are true:

- The maximum achievable efficiency η_{max} monotonically increases with the number of receivers, regardless of the coupling strength between the receivers. Let us consider a numerical example: we consider a CWPT system with N identical receivers, with identical coupling factors k_{0n} between the transmitter and each receiver. The coupling between the different receivers differs from each other. The extended kQ-product α_n for all receivers equals 5. With only one receiver, a maximum attainable efficiency of 67% is possible. Adding a second and third receiver increases η_{max} to 75 and 79%, respectively. Figure 5 depicts η_{max} as a function of the number of identical receivers with $\alpha_n = 5$. It is important to note that the optimal loads for the receivers change depending on the number of receivers in the system. An impedance-matching network and communication system are therefore necessary for a CWPT system with a varying number of receivers.
- The higher the coupling factor between the transmitter and each receiver, the higher η_{max}.
- The lower the parasitic conductances $g_{00}, g_{11}, \ldots, g_{NN}$ of the system, the higher η_{max}.

Finally, we verify if our analytical derivation is compatible with the scientific literature on the subject.

If we consider the case for a single receiver (i.e. $N = 1$), the equations (34), (36), and (28) reduce to:

$$G_1^{opt} = g_{11}\sqrt{1 + \alpha_{N=1}^2} \tag{39}$$

$$C_{load,1}^{opt} = 0 \tag{40}$$

$$\eta_{max} = 1 - \frac{2}{1 + \sqrt{1 + \alpha_{N=1}^2}} \tag{41}$$

with

$$\alpha_{N=1} = \frac{b_{01}}{\sqrt{g_{00}g_{11}}}. \tag{42}$$

The above equations correspond to the expressions found in the literature for $N = 1$ [36, 42]. Note that the optimal load is purely real since no load capacitance is necessary to compensate for the coupling between different receivers (there is only one receiver).

If we consider the case for two coupled receivers (i.e. $N = 2$), the equations (34), (36), and (28) reduce to:

$$G_1^{opt} = g_{11}\sqrt{1 + \alpha_{N=2}^2} \tag{43}$$

$$G_2^{opt} = g_{22}\sqrt{1 + \alpha_{N=2}^2} \tag{44}$$

$$C_{load,1}^{opt} = \frac{g_{11}}{b_{01}\omega_0}\frac{b_{02}b_{12}}{g_{22}} \tag{45}$$

$$C_{load,2}^{opt} = \frac{g_{22}}{b_{02}\omega_0}\frac{b_{01}b_{12}}{g_{11}} \tag{46}$$

$$\eta_{max} = 1 - \frac{2}{1 + \sqrt{1 + \alpha_{N=2}^2}} \tag{47}$$

with

$$\alpha_{N=2}^2 = \frac{b_{01}^2}{g_{00}g_{11}} + \frac{b_{02}^2}{g_{00}g_{22}}. \tag{48}$$

The above equations correspond to the expressions found in the literature for $N = 2$ [43]. The same values for as well the optimal load conductances as the load capacitors, necessary to compensate for the cross-coupling, are found. Note that now load capacitances $C_{load,1}^{opt}$ and $C_{load,2}^{opt}$ are necessary to compensate for the coupling between the two receivers.

Numerical verification

We verify the above analytical derivation by numerical circuit simulation for an example CWPT system with one transmitter and three receivers ($N = 3$). A non-negligible coupling between the receivers is present. The system parameters are listed in Table 2.

The coupling factors, resonance inductances at 10 MHz, and extended kQ-products are calculated from equations (3), (4), (23), and (24) (Table 3).

For this system, the optimal load admittances that maximize the efficiency η are calculated from equations (34) and (36). We find the values of Table 4. The maximum efficiency η_{max} of the system that corresponds to this configuration results from equation (28) and equals to 80.7%.

We now simulate the CWPT system in LTspice XVII®. The circuit simulating the given system with one transmitter and three receivers is shown in Fig. 6. We apply the equivalent pi-circuit for the coupled capacitors, valid near resonance [34, 44]. The simulations are executed in the time-domain with a maximum time step of 1 ps.

Table 2. Chosen simulation parameters for a CWPT system with one transmitter and three receivers

Quantity	Value	Quantity	Value (pF)
g_{00}	1.00 mS	C_0	350
g_{11}	1.50 mS	C_1	250
g_{22}	1.75 mS	C_2	225
g_{33}	2.00 mS	C_3	200
C_{01}	150 pF	C_{12}	20
C_{02}	100 pF	C_{13}	10
C_{03}	50 pF	C_{23}	5
f_0	10 MHz		

Table 3. Calculated simulation parameters for the CWPT system with one transmitter and three receivers

Quantity	Value	Quantity	Value
L_0	0.72 µH	α_N	9.31
L_1	1.01 µH	k_{01}	50.7%
L_2	1.13 µH	k_{02}	35.6%
L_3	1.27 µH	k_{03}	18.9%
α_1	7.70	k_{12}	8.4%
α_2	4.75	k_{13}	4.5%
α_3	2.22	k_{23}	2.4%

Table 4. Calculated values for the maximum efficiency configuration

Quantity	Value	Quantity	Value (pF)
G_1^{opt}	14 mS	$C_{load,1}^{opt}$	14
G_2^{opt}	16 mS	$C_{load,2}^{opt}$	37
G_3^{opt}	19 mS	$C_{load,3}^{opt}$	51
η_{max}	80.7%		

We perform six simulation scenarios with a varying load to verify that the maximum efficiency is achieved for the optimal calculated values from Table 4. In each scenario, we keep all the optimal load admittances (conductances and capacitances) fixed at their optimal value, listed in Table 4, with the exception of one which we vary.

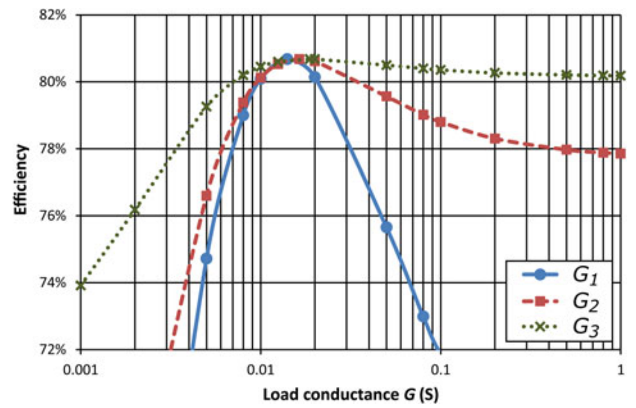

Fig. 7. The simulated efficiency η as a function of varying load conductance for the given system of one transmitter and three receivers. One of the three load conductances is varied, while keeping the other two fixed at their optimal value for maximum efficiency.

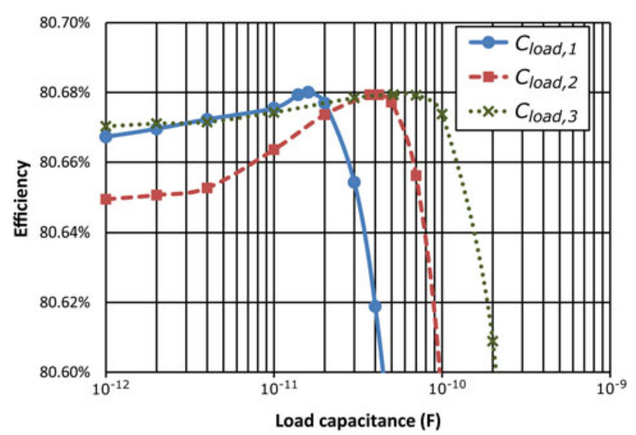

Fig. 8. The simulated efficiency η as a function of varying load capacitor for the given system of one transmitter and three receivers. One of the three load capacitors is varied, while keeping the other two fixed at their optimal value for maximum efficiency.

Figure 7 shows the result for varying conductance: each line shows the simulated efficiency for one varying load conductance. We find that the maximum efficiency is reached for the optimal conductances from Table 4. Additionally, the simulated

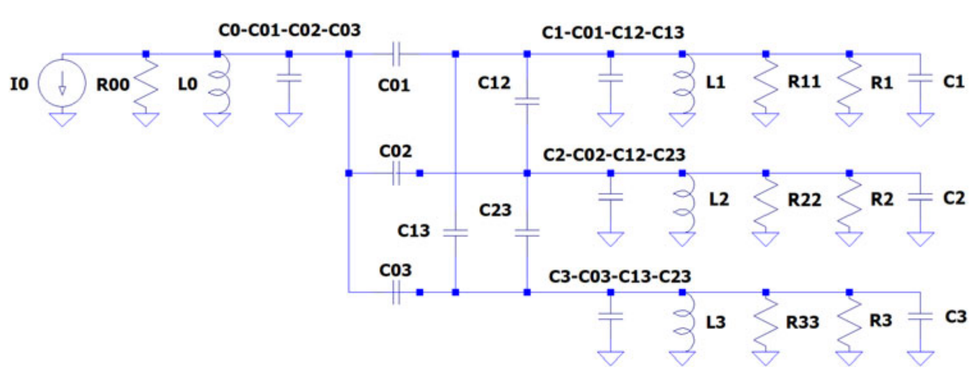

Fig. 6. The circuit in LTspice simulating a system with one transmitter and three receivers. The resistances R_{ii} are applied for the corresponding conductances g_{ii} (i = 0, 1, 2, 3). The coupled capacitors are represented by the equivalent pi-circuits. R_n and C_n (n = 1, 2, 3) depict the load resistances and load susceptances.

values for the maximum efficiency correspond to the analytically calculated value.

Figure 8 shows the simulation results for the other three scenarios for varying load capacitances. Again, all loads are fixed at their optimal value, with the exception of one varying load capacitance. The simulation results verify the calculated values: for the optimal calculated loads of Table 4, the efficiency achieves its maximum value.

We note the non-uniform power distribution in this example: most power (68% of the output power) is delivered to the first receiver, 26% of the output power is supplied to the second receiver, and merely 6% to the third receiver.

Finally, we simulate the system with no coupling present between the receivers, i.e. $C_{12} = C_{13} = C_{23} = 0$. As expected, we find the same values for the optimal load conductances that maximize the efficiency, which illustrates that the load capacitances compensate for the cross-coupling between the receivers. As future work, detailed experimental studies with multiple receivers are required to further study the accuracy of our analytical model.

Conclusion

We studied a CWPT system with an arbitrary number of receivers N. By impedance matching, the power gain or system efficiency can be maximized. We analytically solved the maximum efficiency problem by determining closed-form expressions for the optimal loads of the different receivers, as a function of the couplings and the characteristics of the WPT network.

Both the optimal load conductance G_n^{opt} and load capacitance $C_{load,n}^{opt}$ of receiver n are proportionate to the parasitic conductance g_{nn} of the nth receiver. As well for coupled as uncoupled receivers, the optimal conductances G_n^{opt} assume the same value and are independent on the coupling between the receivers.

We found that capacitors can be inserted into the network as load susceptances to compensate for any cross-coupling between different receivers. The cross-coupling between the receivers does not influence the maximum efficiency η_{max}.

The maximum achievable efficiency η_{max} monotonically increases with the number of receivers, regardless of the coupling strength between the receivers. We expressed this efficiency as a function of a single variable, the extended system kQ-product α_N, which depends on the coupling between the transmitter and each receiver, but is independent on the coupling between the receivers mutually. Its square equals the sum of the squares of the kQ-product of each individual transmitter–receiver link. The higher α_N, the higher the maximum efficiency.

Finally, the analytical derivation was validated by numerical circuit simulation for an example system with three receivers. Measurements on a CWPT setup with multiple receivers are required to confirm the accuracy of the analytical results and are part of future research.

Financial support. This research received no specific grant from any funding agency, commercial or not-for-profit sectors.

Conflict of interest. None.

References

1. **Trevisan R and Costanzo A** (2014) State-of-the-art of contactless energy transfer (CET) systems: design rules and applications. *Wireless Power Transfer* **1**, 10–20.
2. **Lu X, Wang P, Niyato D, Kim DI and Han Z** (2016) Wireless charging technologies: fundamentals, standards, and network applications. *IEEE Communications Surveys and Tutorials* **18**, 1413–1452.
3. **Jawad AM, Nordin R, Gharghan SK, Jawad HM and Ismail M** (2017) Opportunities and challenges for near-field wireless power transfer: a review. *Energies* **10**, 1022.
4. **Kithany D and Markides M** (2019) Wireless Power Market Tracker. IHS Markit, London, UK, Rep. Q1-2019.
5. **Fu M, Zhang T, Ma C and Zhu X** (2015) Efficiency and optimal loads analysis for multiple-receiver wireless power transfer systems. *IEEE Transactions on Microwave Theory and Techniques* **63**, 801–812.
6. **Liu X, Wang G and Ding W** (2014) Efficient circuit modelling of wireless power transfer to multiple devices. *IET Power Electronics* **7**, 3017–3022.
7. **Kim J, Kim DH and Park YJ** (2014) Analysis of capacitive impedance matching networks for simultaneous wireless power transfer to multiple devices. *IEEE Transactions on Industrial Electronics* **62**, 2807–2813.
8. **Fu M, Zhang T, Zhu X, Luk PCK and Ma C** (2016) Compensation of cross coupling in multiple-receiver wireless power transfer systems. *IEEE Transactions on Industrial Informatics* **12**, 474–482.
9. **Sugiyama R, Duong QT and Okada M** (2017) kQ-product analysis of multiple-receiver inductive power transfer with cross-coupling. *International Workshop on Antenna Technology: Small Antennas, Innovative Structures, and Applications (iWAT)*, Athens, Greece, 2017.
10. **Duong QT and Okada M** (2016) Maximum efficiency formulation for inductive power transfer with multiple receivers. *IEICE Electronics Express* **13**, 20160915.
11. **Monti G, Che W, Wang Q, Dionigi M, Mongiardo M, Perfetti R and Chang Y** (2016) Wireless power transfer between one transmitter and two receivers: optimal analytical solution. *Wireless Power Transfer* **3**, 63–73.
12. **Lu F, Zhang H and Mi C** (2017) A review on the recent development of capacitive wireless power transfer technology. *Energies* **10**, 1752.
13. **Lu F, Zhang H and Mi C** (2018) A two-plate capacitive wireless power transfer system for electric vehicle charging applications. *IEEE Transactions on Power Electronics* **33**, 964–969.
14. **Li S, Liu Z, Zhao H, Zhu L, Shuai C and Chen Z** (2016) Wireless power transfer by electric field resonance and its application in dynamic charging. *IEEE Transactions on Industrial Electronics* **63**, 6602–6612.
15. **Zhang H, Lu F, Hofmann H, Liu W and Mi CC** (2016) A four-plate compact capacitive coupler design and LCL-compensated topology for capacitive power transfer in electric vehicle charging application. *IEEE Transactions on Power Electronics* **31**, 8541–8551.
16. **Komaru T and Akita H** (2013) Positional characteristics of capacitive power transfer as a resonance coupling system. *IEEE Wireless Power Transfer (WPT)*, May 2013.
17. **Zhang H, Lu F, Hofmann H, Liu W and Mi CC** (2017) Six-plate capacitive coupler to reduce electric field emission in large air-gap capacitive power transfer. *IEEE Transactions on Power Electronics* **33**, 665–675.
18. **Rozario D, Azeez NA and Williamson SS** (2016) Comprehensive review and comparative analysis of compensation networks for capacitive power transfer systems. *IEEE 25th International Symposium on Industrial Electronics (ISIE)*, 2016.
19. **Kumar A, Pervaiz S, Chang CK, Korhummel S, Popovic Z and Afridi KK** (2015) Investigation of power transfer density enhancement in large air-gap capacitive wireless power transfer systems. *IEEE Wireless Power Transfer Conference*, 2015.
20. **Mi C** (2015) High power capacitive power transfer for electric vehicle charging applications. *The 6th IEEE International Conference on Power Electronics Systems and Applications (PESA)*, Hong Kong, China, 2015.
21. **Karabulut A, Bilic HG and Ozdemir S** (2018) Capacitive Power Transfer Theory and the Overview of its Potential. *3rd International Mediterranean Science and Engineering Congress*, Adana, Turkey, 2018.
22. **Huang L, Hu P, Swain A and Su YZ** (2016) Impedance compensation for wireless power transfer based on electric field coupling. *IEEE Transactions on Power Electronics* **33**, 7556–7563.
23. **Xia C, Zhou Y, Zhang J and Li C** (2012) Comparison of power transfer characteristics between CPT and IPT system and mutual inductance optimization for IPT system. *Journal of Computers* **7**, 2734–2741.

24. **Culurciello E and Andreou AG** (2006) Capacitive inter-chip data and power transfer for 3-D VLSI. *IEEE Transactions on Circuits and Systems II: Express Briefs* **53**, 1348–1352.
25. **Mostafa T, Muharam A and Hattori R** (2017) Wireless battery charging system for drones via capacitive power transfer. *Proceedings of the IEEE Workshop on Emerging Technologies: Wireless Power Transfer*, Chongqing, China, 2017.
26. **Hu AP, Liu C and Li H** (2008) A novel contactless battery charging system for soccer playing robot. *Proceedings of the International Conference on Mechatronics and Machine Vision in Practice*, Auckland, New Zealand, 2008.
27. **Theodoridis MP** (2012) Effective capacitive power transfer. *IEEE Transactions on Power Electronics* **27**, 4906–4913.
28. **Sodagar A and Amiri P** (2009) Capacitive coupling for power and data telemetry to implantable biomedical microsystems. *Proceedings of the IEEE Conference on Neural Engineering*, Antalya, Turkey, 2009.
29. **Jegadeesan R, Agarwal K, Guo Y, Yen S and Thakor N** (2017) Wireless power delivery to flexible subcutaneous implants using capacitive coupling. *IEEE Transactions on Microwave Theory and Techniques* **65**, 280–292.
30. **Dai J and Ludois DC** (2015) Wireless electric vehicle charging via capacitive power transfer through a conformal bumper. *Proceedings of the IEEE Applied Power Electronics Conference and Exposition (APEC)*, Charlotte, NC, USA, 2015.
31. **Miyazaki M, Abe S, Suzuki Y, Sakai N, Ohira T and Sugino M** (2017) Sandwiched parallel plate capacitive coupler for wireless power transfer tolerant of electrode displacement. *Proceedings of the IEEE MTT-S International Conference on Microwaves for Intelligent Mobility (ICMIM)*, Nagoya, Japan, 2017.
32. **Kim G, Boo S, Kim S and Lee B** (2018) Control of power distribution for multiple receivers in SIMO wireless power transfer system. *Journal of Electromagnetic Engineering and Science* **18**, 221–230.
33. **Huang L and Hu AP** (2015) Defining the mutual coupling of capacitive power transfer for wireless power transfer. *Electronics Letters* **51**, 1806–1807.
34. **Hong JSG and Lancaster MJ** (2001) *Microstrip Filters for RF/Microwave Applications*, 1st Edn. New York, NY, USA: John Wiley & Sons, pp. 235–253.
35. **Minnaert B and Stevens N** (2017) Conjugate image theory applied on capacitive wireless power transfer. *Energies* **10**, 46.
36. **Kracek J and Svanda M** (2018) Analysis of capacitive wireless power transfer. *IEEE Access* **7**, 26678–26683.
37. **Boyd S and Vandenberghe L** (2004) *Convex Optimization*, 2nd Edn. Cambridge: Cambridge University Press, p. 140.
38. **Minnaert B and Stevens N** (2017) Single variable expressions for the efficiency of a reciprocal power transfer system. *International Journal of Circuit Theory and Applications* **10**, 1418–1430.
39. **Ohira T** (2014) Extended k-Q product formulas for capacitive-and inductive-coupling wireless power transfer schemes. *IEICE Electronics Express* **11**, 20140147.
40. **Ujihara T, Duong QT and Okada M** (2017) kQ-product analysis of inductive power transfer system with two transmitters and two receivers. *IEEE Wireless Power Transfer Conference*, Taipei, Taiwan, 2017.
41. **Duong QT and Okada M** (2017) kQ-product formula for multiple-transmitter inductive power transfer system. *IEICE Electronics Express* (2017), 14-20161167.
42. **Dionigi M, Mongiardo M, Monti G and Perfetti R** (2017) Modelling of wireless power transfer links based on capacitive coupling. *International Journal of Numerical Modelling: Electronic Networks, Devices and Fields* **30**, e2187.
43. **Minnaert B and Stevens N** (2017) Optimal analytical solution for a capacitive wireless power transfer system with one transmitter and two receivers. *Energies* **10**, 1444.
44. **Montgomery CG, Dicke RH and Purcell EM** (1948) *Principles of Microwave Circuits*. York, PA: IET.

Ben Minnaert obtained his PhD in Engineering in 2007 at Ghent University, Belgium. He authored or co-authored more than 50 papers on international journals and conferences. In 2018, he obtained a permanent position as researcher and lecturer at the University College Odisee, KU Leuven Association. His main research interest is the modelling of energy systems, including energy harvesting, photovoltaic solar cells, and wireless power transfer. Recently, he has developed near-field wireless power transfer systems for non-static applications. His research activities are dedicated to embedded systems, wireless sensor networks, IoT-applications, and (inductive and capacitive) wireless power transfer for multiple transmitters and receivers.

Mauro Mongiardo (F'11) has received the Laurea degree (110/110 cum laude) in Electronic Engineering from the University of Rome "La Sapienza" in 1983. In 1991, he became an Associate Professor of Electromagnetic Fields, and from 2001, he is a full Professor of Electromagnetic Fields at the University of Perugia. He has been elected Fellow of the IEEE "for contributions to the modal analysis of complex electromagnetic structures" in 2011. The scientific interests of Mauro Mongiardo have concerned primarily the numerical modeling of electromagnetic wave propagation both in closed and open structures. His research interests have involved CAD and optimization of microwave components and antennas.

Mauro Mongiardo has served in the Technical Program Committee of the IEEE International Microwave Symposium from 1992. From 1994, he is a member of the Editorial Board of the *IEEE Transactions on Microwave Theory and Techniques*. During the years 2008–2010, he has been an Associate Editor of the *IEEE Transactions on Microwave Theory and Techniques*. He is an author or co-author of over 200 papers and articles in the fields of microwave components, microwave CAD, and antennas. He is the co-author of the books *Open Electromagnetic Waveguides* (IEE, 1997) and *Electromagnetic Field Computation by Network Methods* (Springer, 2009).

Alessandra Costanzo (A'99–M'02–SM'13) is full professor at the University of Bologna, Italy. Her research activities are dedicated to CAD algorithms for multi-domain co-design and modeling of active nonlinear microwave/RF circuits. Recently she has proposed novel solutions for energy autonomous RF systems based on the wireless power transmission, adopting both far-field and near-field solutions, for several power levels and operating frequencies. She has authored more than 240 scientific publications on peer-reviewed international journals and conferences and several chapter books. Dr. Costanzo is a co-founder of the EU COST Action IC1301 WiPE Wireless Power Transfer for Sustainable Electronics, where she chaired WG1: Far-Field Wireless Power Transfer. She is past-chair of the MTT-26 Committee on Wireless Energy Transfer and Conversion and a member of the MTT-24 Committee on RFID. Since 2016, she has been the Steering Committee Chair of the new *IEEE Journal of Radio Frequency Identification*. She is the MTT-S representative and Distinguished Lecturer of the Council on Radio Frequency Identification (CRFID). She serves as an Associate Editor for the *IEEE Transactions on Microwave Theory And Techniques*, the *Cambridge International Journal of Microwave and Wireless Technologies*, and the *Cambridge International Journal of Wireless Power Transfer*. She is IEEE senior member.

Franco Mastri received the laurea degree (with honors) in Electronic Engineering from the University of Bologna, Bologna, Italy, in 1985. In 1990, he become a Research Associate with the Istituto di Elettrotecnica, University of Bologna, and since 2005 he has been an Associate Professor of Electrotechnics with the Department of Electrical, Electronic, and Information Engineering "Guglielmo Marconi," University of Bologna. His research interests include nonlinear-circuit simulation and design techniques, nonlinear RF device modeling, stability and noise analysis of nonlinear circuits, nonlinear/electromagnetic co-simulation of RF systems, and systems for wireless power transmission. He authored or co-authored four book chapters and about 140 papers on international journals and conferences.